Environ Fluid Mech (2012) 12:265–289
DOI 10.1007/s10652-011-9234-z

ORIGINAL ARTICLE

Turbulence measurements in a small subtropical estuary under king tide conditions

Hubert Chanson · Richard Brown · Mark Trevethan

Received: 3 October 2011 / Accepted: 27 December 2011 / Published online: 11 January 2012
© Springer Science+Business Media B.V. 2012

Abstract In natural waterways and estuaries, the understanding of turbulent mixing is critical to the knowledge of sediment transport, stormwater runoff during flood events, and release of nutrient-rich wastewater into ecosystems. In the present study, some field measurements were conducted in a small subtropical estuary with micro-tidal range and semi-diurnal tides during king tide conditions: i.e., the tidal range was the largest for both 2009 and 2010. The turbulent velocity measurements were performed continuously at high-frequency (50 Hz) for 60 h. Two acoustic Doppler velocimeters (ADVs) were sampled simultaneously in the middle estuarine zone, and a third ADV was deployed in the upper estuary for 12 h only. The results provided an unique characterisation of the turbulence in both middle and upper estuarine zones under the king tide conditions. The present observations showed some marked differences between king tide and neap tide conditions. During the king tide conditions, the tidal forcing was the dominant water exchange and circulation mechanism in the estuary. In contrast, the long-term oscillations linked with internal and external resonance played a major role in the turbulent mixing during neap tides. The data set showed further that the upper estuarine zone was drastically less affected by the spring tide range: the flow motion remained slow, but the turbulent velocity data were affected by the propagation of a transient front during the very early flood tide motion at the sampling site.

Keywords Turbulence · Small subtropical estuary · Micro-tidal estuary · Turbulent mixing · King tides · Middle estuary · Upper estuary · Acoustic Doppler velocimetry · Transient front

H. Chanson (✉)
School of Civil Engineering, The University of Queensland, Brisbane, QLD 4072, Australia
e-mail: h.chanson@uq.edu.au
URL: http://www.uq.edu.au/~2hchans/

R. Brown
School of Engineering Systems, Queensland University of Technology, Brisbane, QLD 4000, Australia

M. Trevethan
Natural-Systems Research Group, Elwood, VIC 3184, Australia

1 Introduction

In natural estuaries, the understanding of turbulent mixing is critical to the modelling of sediment transport, storm-water runoff during flood events, and release of nutrient-rich wastewater into ecosystems [34,36]. The predictions of contaminant transport and mixing in the estuarine zone are challenging because of the limited understanding of the turbulence fundamentals and limited validation data sets: "The fate and transport of pollutants within […] the freshwater-intertidal, the saline-intertidal and the estuary as a whole needs further study in relation to flux estimation and discharge" [18]. Long-duration studies of the properties of turbulence at high frequency are limited. Most data lacked spatial and temporal resolution to gain insight into the characteristics of fine-scale turbulence: e.g. [1,35,13,28,37]. A majority of studies were conducted for relatively short periods (up to 6 h) [2,38] and/or by collecting data over long periods in bursts of several minutes [24]. A few investigations performed some continuous, high frequency sampling of a full tidal cycle or longer, although mainly for neap tide conditions [32].

A series of studies were conducted in a small subtropical estuary with micro-tidal conditions (Table 1) [33]. The combined results showed that the bulk flow properties varied in time with periods comparable to tidal cycles, while the turbulence properties depended upon the instantaneous local properties. A striking feature of all data sets was the large fluctuations in all turbulence parameters during the tidal cycle including at slacks. The studies were undertaken with tidal ranges between 1.36 and 2.53 m, and the bulk of the data were obtained under neap tides.

In the present study, some detailed turbulence field measurements were conducted continuously at high-frequency (50 Hz) for 60 h in a small subtropical estuary with semi-diurnal tides during king tide conditions: i.e., the tidal range was the largest for both 2009 and 2010. Two acoustic Doppler velocimeters (ADVs) were sampled simultaneously at two fixed vertical elevations in the middle estuarine zone for the entire study duration. A third acoustic Doppler velocimeter was deployed in the upper estuary for 12 h within the study period. The results characterised the turbulence and turbulent mixing processes in both the middle and upper estuarine zones under the large spring tides. The field investigation and instrumentation are described in the next section. The main results are presented in the later sections.

2 Study site and instrumentation

2.1 Presentation

The field study was conducted in the small subtropical estuary of Eprapah Creek in eastern Australia (Redlands, QLD) under king tide conditions. The estuarine zone is 3.8 km long, about 1–2 m deep mid-stream, and about 20–30 m wide (Fig. 1). Figure 1b presents a number of cross-sectional surveys at several longitudinal locations along the estuary, where AMTD means the adopted middle thread distance measured upstream from the river mouth. The Eprapah Creek estuary has been monitored for 30 years, and several detailed field experiments have been conducted since 2003 although mostly under neap tide conditions [4,7,31–33] (Table 1). The catchment area is about 40 km^2 and the creek flows directly into Moreton Bay, off the Pacific Ocean. The estuary is a drowned river valley type with a wet and dry tropical/subtropical hydrology, and some small, sporadic freshwater inflows. This is a relatively small, narrow, elongated and meandering estuary with a cross-section which deepens and widens towards the mouth, surrounded by extensive mud flats. For an alluvial river such

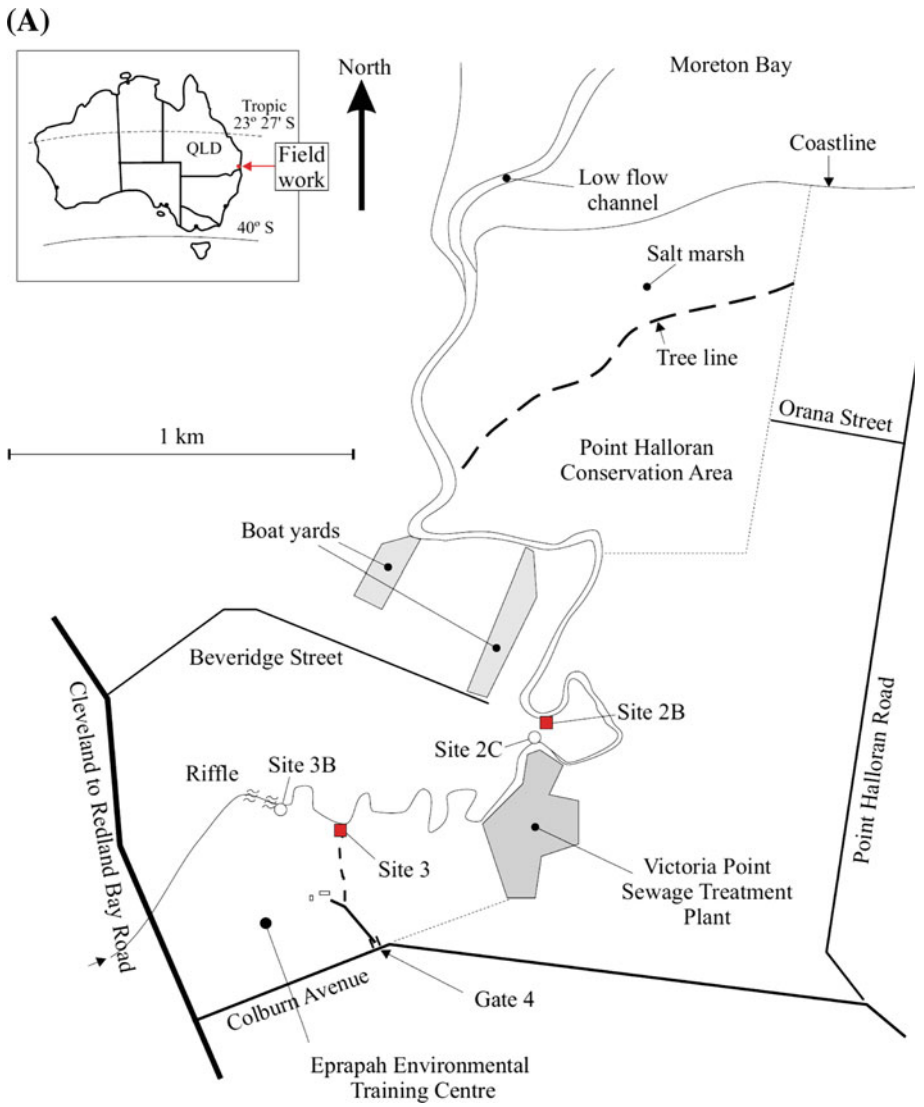

Fig. 1 Estuarine zone of Eprapah Creek, Australia. **a** General map based upon an aerial photograph. **b** Surveyed cross-sections (looking downstream). From *top to bottom* AMTD 0.3, 2.1 km (Site 2B) and 3.1 km (Site 3). *Dotted line* Mean Sea Level. Surveys conducted on 1–2 February 2010. The surveys stopped in the mangrove trees

as Eprapah Creek, the channel cross-section area A decays exponentially with increasing distance from the river mouth:

$$A = A_o \times \exp\left(-\frac{x'}{a}\right) \tag{1}$$

where A_o is the cross-section area at the river mouth, x' is the longitudinal distance from the river mouth positive upstream and a is the convergence length [25,26]. At Eprapah Creek,

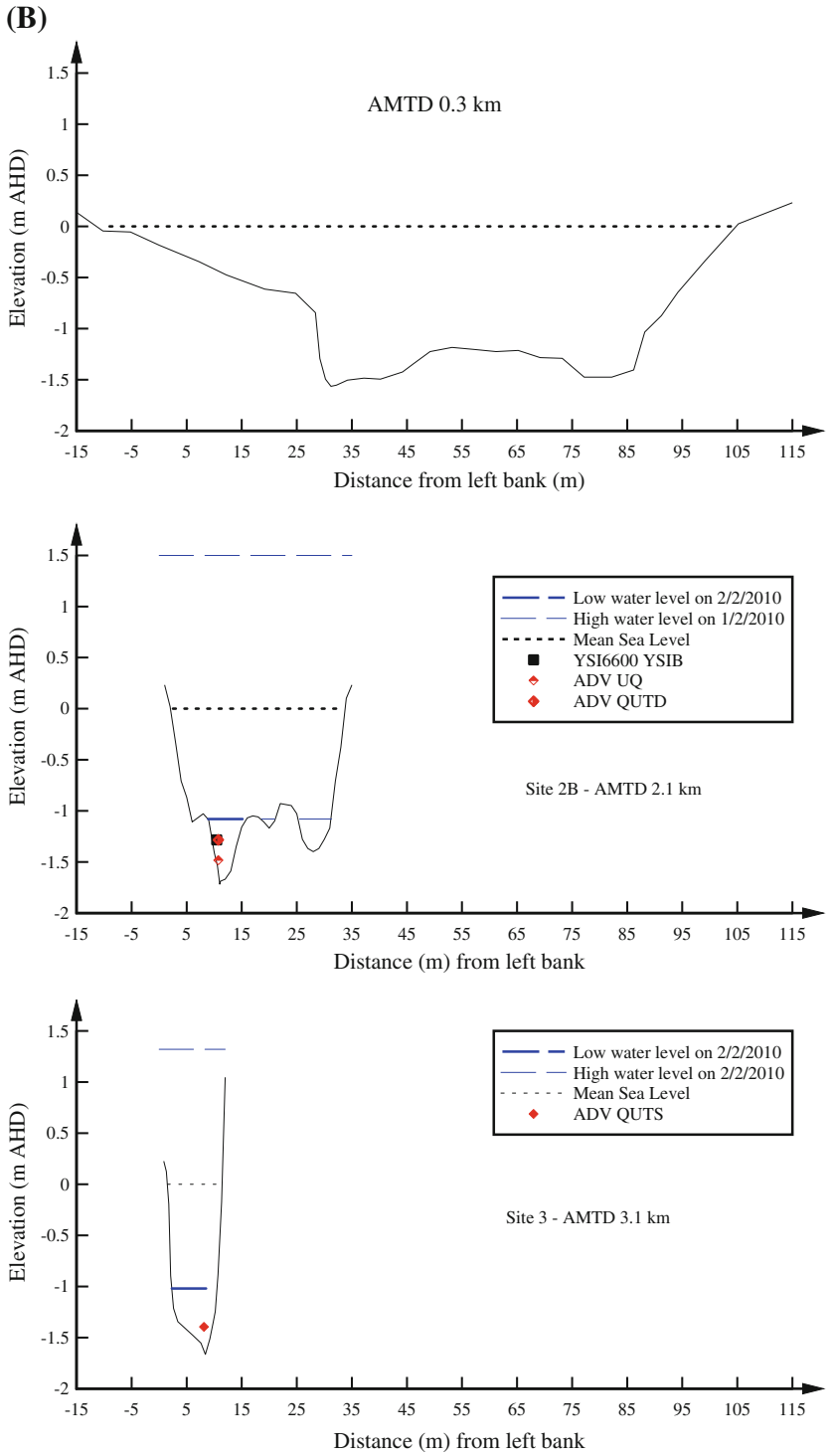

Fig. 1 contined

Table 1 Turbulence field measurements at Eprapah Creek QLD, Australia

Study (1)	Dates (2)	Tidal range (m) (3)	ADV system(s) (MHz) (4)	Sampling rate (Hz) (5)	Sampling duration (6)	Sampling volume location(s) (7)
E1	4/04/03	1.84	10	25	9 × 25 min	AMTD 2.1 km, 14.2 m from left bank, 0.5 m below surface
E2	17/07/03	2.03	10	25	8 h	AMTD 2.0 km, 7.7 m from left bank, 0.5 m below surface
E3	24/11/03	2.53	10	25	7 h	AMTD 2.1 km, 10.7 m from left bank, 0.5 m below surface
E4	2/09/04	1.81	10	25	6 & 3 h	AMTD 2.1 km, 10.7 m from left bank, 0.052 m above bed
E5	8–9/03/05	2.37	10	25	25 h	AMTD 2.1 km, 10.7 m from left bank, 0.095 m above bed
E6	16–18/05/05	1.36	10 & 16	25	49 h	AMTD 2.1 km, 10.7 m from left bank, 0.2 & 0.4 m above bed
E7	5–7/06/06	1.58	10 & 16	25 & 50	50 h	AMTD 3.1 km, 4.2 m from right bank, 0.2 & 0.4 m above bed
E8	28/08/06	2.10	–	–	12 h	Surface velocity data. AMTD 1.0, 2.1 & 3.1 km
E10	6–8/06/07	1.76	16	50	50 h	AMTD 2.1 km, 10.7 m from left bank, 0.13 & 0.38 m above bed
E11	31/1/10–3/02/10	2.78	16	50	60 h	Site 2B: AMTD 2.1 km, 10.75 m from left bank, 0.12 & 0.32 m above bed Site 3: AMTD 3.1 km, 3.85 m from right bank, 0.235 m above bed

Note AMTD Adopted Middle Thread Distance measured upstream from river mouth

the detailed surveys of the channel cross-section yielded $A_o = 109.2\,m^2$ and a = 0.655 km at mean sea level.

The present field study E11 was conducted under king tide conditions from 31 January to 3 February 2010. The tidal range was the largest for both 2009 and 2010 (Table 1, column 3). Although the tides are semi-diurnal, the tidal cycles have slightly different periods and amplitudes indicating some diurnal inequality (Fig. 2). In Fig. 2, the free-surface measurements at middle estuary site 2B and upper estuary site 3 are compared with water levels recorded at the Brisbane River bar located 25 km NNW of the mouth of Eprapah Creek. The water elevations are presented in m AHD, where AHD stands for Australian Height Datum or Mean Sea Level. During the present study, some continuous high-frequency turbulence and physio-chemical data were recorded mid-estuary at Site 2B for 60 h. In addition, some continuous, high-frequency sampling was conducted for 12 h in the upper estuary at Site 3 on 2 February 2010. Both Sites 2B and 3 are highlighted with a red square in Fig. 1a.

The weather was overcast for the entire study period with a few short showers. The air temperatures ranged from 21 to 32°C. Approximately 25 mm of rain fell over the estuary:

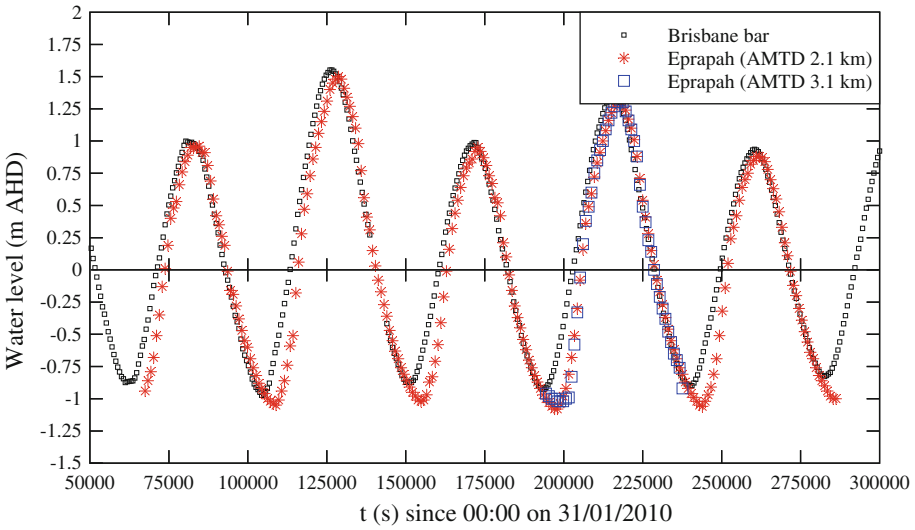

Fig. 2 Measured water depths at Eprapah Creek on 31 January, 1, 2 and 3 February 2010. Time since 00:00 on 31 January 2010. Comparison with the measured water depths at Brisbane bar (Courtesy of Tidal Unit Maritime Safety Queensland-Brisbane)

i.e., 6, 6.5, 2.5 and 10 mm were recorded at the Victoria Point sewage treatment plant on 31 January, 1 February, 2 February and 3 February 2010 respectively. The location of the Victoria Point sewage treatment plant is shown in Fig. 1a.

2.2 Instrumentation

For this field investigation, three Sontek^{TM} microADVs and two YSI6600 probes were deployed. Two microADVs and both YSI6600 probes were installed mid-estuary at Site 2B, approximately 10.7 m from the left bank. The YSI6600 probes were multi-parameter probes, and the simultaneous measurements included conductivity, temperature, turbidity, pH, dissolved oxygen (DO), and chlorophyll A levels. The two microADVs were located at 10.75 m from the left bank, and at 0.12 and 0.32 m above the bed. Their sampling volumes were aligned vertically, and the ADVs were sampled continuously at 50 Hz. A YSI6600 probe was located 0.32 m above the bed and 0.30 m beside the upper microADV. The second YSI6600 probe was mounted on a float and the sensors were located 0.2 m below the surface. Both YSI6600 probes were sampled at 0.083 Hz. The third ADV was deployed in the upper estuary at Site 3 on 2 February 2010 for 12 h and sampled at 50 Hz. The location of the sampling volumes in the experimental cross-sections is shown in Fig. 1b. All ADV data underwent a thorough post-processing procedure to eliminate any erroneous or corrupted data. The post-processing technique was described in [8].

In addition of the three velocity components, the ADV signal outputs included the ADV signal strength which is proportional to the number of particles in the ADV sampling volume. Herein the acoustic backscatter intensity (BSI) was used and it is a function of the ADV signal strength:

$$I_b = 10^{-5} \times 10^{0.043\text{Ampl}} \quad (2)$$

where the BSI I_b is dimensionless and the average ADV signal amplitude (Ampl) is in counts. The coefficient 10^{-5} is a value introduced to avoid large values of BSI. The acoustic BSI may be used as a proxy for the instantaneous suspended sediment concentration (SSC) because of the strong relationship between I_b and SSC [9,21].

Some vertical profiles of water quality parameters were conducted on 1 February 2010 with a YSI6920 probe. The measurements were conducted on the channel centreline between (HW + 1h) and (LW − 3h), where HW is the high water and LW is the low water. In addition, some surface sampling was conducted at Site 3 on 2 February 2010 between 06:00 and 18:00. The measurements included surface velocity direction, air and water temperature, turbidity (Secchi disk), and conductivity. The air temperature was measured with an alcohol thermometer. Water conductivity and temperature were recorded with Oaklon^{TM} ECTest High+ thermometer/conductivity meters. The water elevations were measured with a graduated pole installed at the low tide at both sites. The water turbidity was measured with a 30 cm diameter Secchi disk. The surface water samples were taken at 0.1–0.2 m below the surface.

2.3 Data accuracy

The accuracy of the velocity measurements was 1% of the velocity range, whilst the physio-chemical probes YSI6600 and YSI6920 gave a data accuracy of ±0.5% for conductivity, ±0.15°C for temperature, ±5% for turbidity, ±0.2 unit for pH, ±2% of saturation concentration for DO.

3 General observations

3.1 Presentation

The field study was conducted from 31 January to 3 February 2010 in the middle and upper estuarine zones (Fig. 1a). A key feature of the study was the king tide conditions. The water elevation records are presented in Fig. 2. The water level measurements showed the maximum and minimum water levels always after the reference high and low tides at the river mouth (Victoria Point). This is typical of an estuarine system in which the change in boundary conditions at the river mouth must travel upstream [3,11]. The water levels in the estuary were dominated by tidal forcing and little difference in water levels was observed between the two sampling sites (Fig. 2). Some photographs taken at low and high tides are presented in Fig. 3. Further photographs were shown in [10].

The extreme LW and HW levels had some impact on the estuary hydrodynamics with drastic changes in channel cross-sections (Fig. 1b). At low tides, the rock formations in the middle estuary (Site 2B) acted as a weir (Fig. 3a). They created some disruption of the flow motion between the upper and lower estuary. There were further shoals and bars upstream of Site 2B blocking the water exchanges between the upper estuary and the river mouth. In turn, the upper estuarine zone became practically disconnected from the lower estuary, with some potential implications in terms of the sewage treatment plant effluent release. At high tides, the mangroves and surrounding mudflats were inundated. For example, the grass seen in Fig. 3c, d (right) was inundated at high tide and the water surface reached the underside of the platform and boardwalk. During the early ebb tide, the estuary cross-section was characterised by a rapid reduction in flow cross-section when the water level in the creek dropped below the bank edges, and the mangrove swamps and flats trapped some brackish water volumes. These waters were released later during the early to mid-ebb tides.

Fig. 3 Sampling sites 2B and 3 in Eprapah Creek at high and low tides. **a** Sampling site 2B in Eprapah Creek mid-estuary (AMTD 2.1 m). View from the left bank on 1 February 2010 at 06:20 (low tide). Note the rock formations in the channel centreline and the two low flow channels in the foreground and background. The ADV units and YSI6600 units were located in the foreground channel. The second YSI6600 unit was attached to the *blue float* on the left. **b** Sampling site 2B: view from the left bank on 1 February 2010 at 10:20 (end of flood tide). **c** Sampling site 3 in Eprapah Creek upper estuary (AMTD 3.1 km): view from the right bank looking downstream at low tide on 2 February 2010 at 06:20. **d** Sampling site 3: view from the right bank looking downstream at high tide on 2 February 2010 at 11:37

The time-averaged longitudinal velocity data highlighted that the largest ebb and flood velocities occurred about low tide and early flood tide (Fig. 4). Figure 4 shows the time-averaged longitudinal velocity components and the water depth as functions of time for all ADV units at Site 2B (z = 0.12 & 0.32 m above bed) and Site 3 (z = 0.235 m above bed). Here V_x is positive downstream, the transverse component V_y is positive towards the left bank and the vertical velocity component V_z is positive upwards. All the velocity data showed a very rapid flow reversal shortly after low tide. This is illustrated in Fig. 4a. The low tide slack reversal was sudden and the early flood tide current was very intense with a strong upstream current mid-estuary. The largest longitudinal time-averaged velocities were recorded during the very early flood tide. If low tide is defined in terms of the lowest water level, and low tide slack as $\overline{V_x} = 0$, the data showed that low tide slack took place on average 360 and 510 s after low tide for z = 0.12 and 0.32 m respectively.

In the middle estuarine zone, the longitudinal velocity data showed a number of flow reversals around high tide, as well as some long-period oscillations. For example, some long period oscillations are seen in Fig. 4a between t = 72,000 and 104,500 s with a period of about 43 min, where the time t is counted from 00:00 on 31 January 2010. Similar phenomena were observed previously under neap tide conditions at Eprapah Creek [32,33]. The multiple flow reversals and low-frequency velocity oscillations lasted between 40 min and 1.5 h. These were caused by some form of external resonance which was linked with some East-West sloshing mode in Moreton Bay.

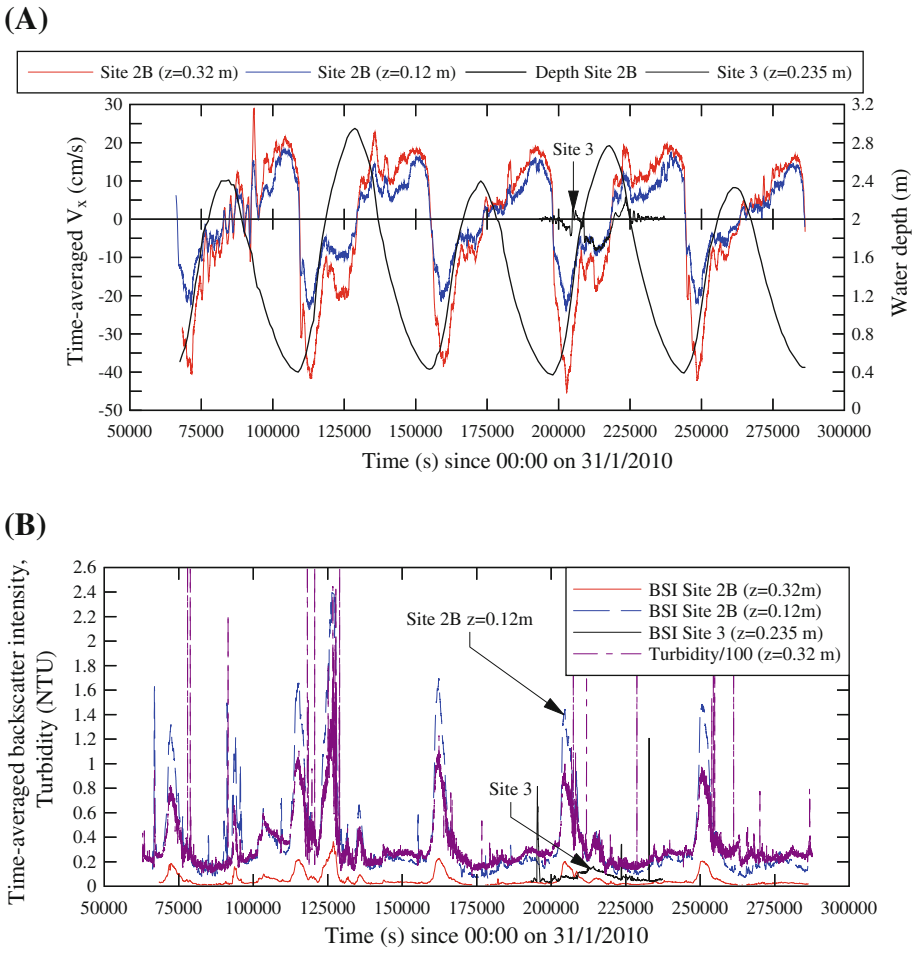

Fig. 4 Water depth, time-averaged velocity components, time-averaged BSI and turbidity as functions of time. Data collected at Sites 2B and 3, Eprapah Creek during the study E11 (31 June–3 February 2010). VITA calculations using the average of the next 10,000 samples (200 s) at 10 s intervals along entire datasets, **a** water depth (Site 2B) and longitudinal velocity V_X and **b** turbidity (Site 2B) and BSI

In the upper estuarine zone (Site 3), the water depth and time-averaged longitudinal velocity were time-dependant and fluctuated, with periods comparable to the tidal cycles and other large-scale processes (Figs. 2, 4a). During the 12 h period corresponding a major tidal cycle, the largest velocity magnitude took place during the second half of the flood tide and first half of the ebb tide, although the magnitude was significantly smaller than that observed mid-estuary (Site 2B) during the same field study (Fig. 4).

Figure 4b shows the time-averaged acoustic BSI at both sites, and the turbidity recorded in the middle estuary at $z = 0.32$ m above the bed. The acoustic backscatter data showed some strong correlation with the turbidity data as seen in Fig. 4b. Both the BSI and turbidity data presented some marked peaks during the early flood tide, when the water depth was low, the flood flow velocity was large and the depth-averaged velocity gradient was the largest. The large depth-averaged velocity gradient was favourable to the erosion and re-suspension of

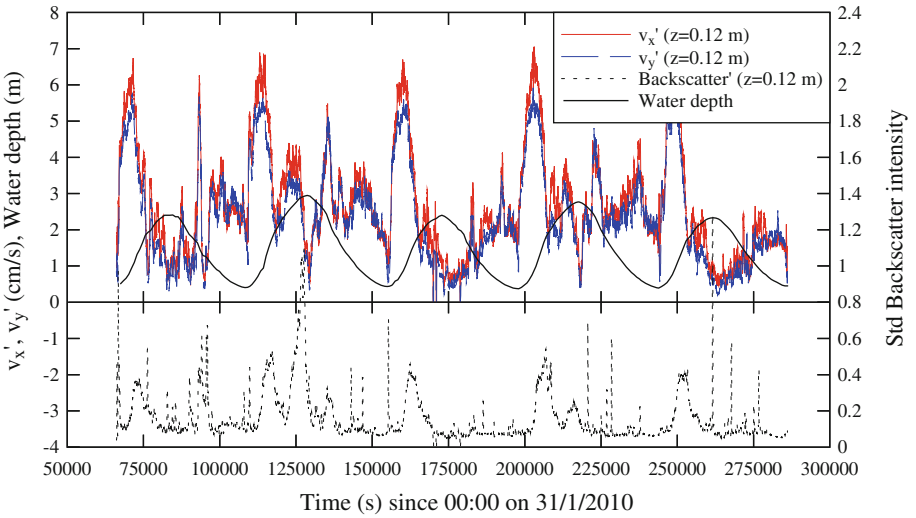

Fig. 5 Water depth, and standard deviations of velocity components and BSI at z = 0.12 m as functions of time as functions of time in the middle estuary. Data collected at Site 2B, Eprapah Creek during the study E11 (31 June–3 February 2010). VITA calculations using the average of the next 10,000 samples (200 s) at 10 s intervals along entire datasets

the bed material. The findings were consistent with an earlier study conducted at the same site under neap tide conditions [9,32].

The standard deviation of the turbulent velocity components represents the magnitude of turbulent velocity fluctuations. The middle estuary data are presented in Fig. 5. During the field study, the standard deviations of all velocity components were the largest during the first half of the flood tide. A second period of large standard deviations of all velocity components was the early ebb tide. It is believed that the latter was linked to the emptying of the inundated mangroves and surrounding mudflats into the main channel which induced some strong stirring and mixing of the water column in the main channel. The horizontal and vertical turbulence intensities v'_y/v'_x and v'_z/v'_x showed no discernable tidal trend for all ADV units. In the middle estuary (Site 2B), v'_y/v'_x was equal to 0.87 and 0.92 on average at z = 0.12 and 0.32 m respectively, while v'_z/v'_x equalled 0.75 on average at z = 0.32 m. In the upper estuary, $v'_y/v'_x = 0.75$ and $v'_z/v'_x = 0.60$ on average at z = 0.235 m. The middle estuary findings were close to the data recorded during the studies E5 and E6 (Table 1) at the same middle estuarine site 2B with neap and spring tide conditions respectively. The results tended overall to yield larger ratios of v'_y/v'_x and v'_z/v'_x than those observed in laboratory studies with straight prismatic rectangular channels [14,19,20].

Figure 5 includes the standard deviation of the acoustic BSI. The present experimental results showed some large fluctuations in acoustic BSI during the flood tide (Fig. 5). There was a solid correlation between the standard deviations of all velocity components and the standard deviation of the BSI, showing the inter-relation between suspended sediment motion and turbulence. In Fig. 5, the BSI standard deviation data at z = 0.12 m included a number of spikes that might reflect some sediment pickup by turbulent bursts next to the bed.

It is noteworthy that the present data set obtained in king tide conditions showed some marked differences with neap tide conditions. In the present study, the tidal forcing was the

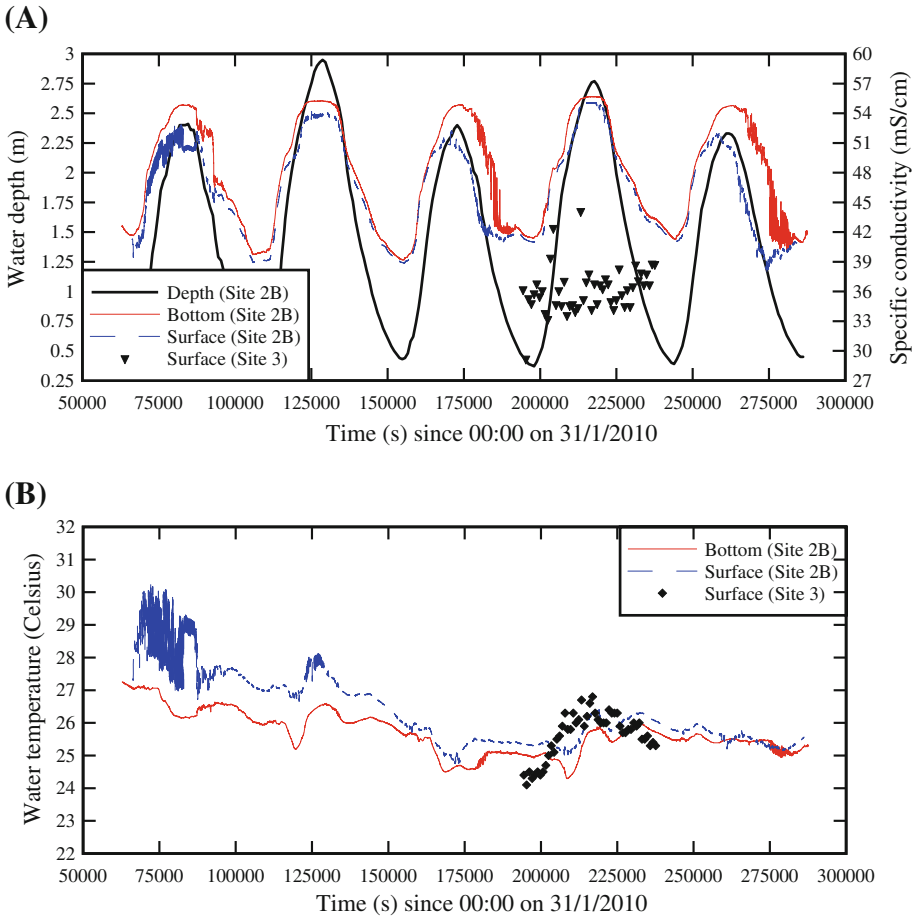

Fig. 6 Water depth, conductivity, temperature, pH and chlorophyll A as functions of time. Data collected by the YSI6600 units at Site 2B, Eprapah Creek during the study E11 (31 January–3 February 2010). Comparison with surface measurements at Site 3 on 2 February 2010. **a** Water depth (Site 2B) and specific conductivity at Sites 2B and 3. **b** Bottom and surface water temperatures at Sites 2B and 3. **c** Chlorophyll A (Site 2B) and air temperatures at Sites 2B and 3. **d** pH at Site 2B

dominant water exchange and circulation mechanism in the estuary. In contrast, the long-term oscillations linked with internal and external resonance played a major role in the turbulent mixing during neap tide conditions [31–33].

3.2 Physio-chemical properties

The water temperature, conductivity, turbidity, pH, DO and chlorophyll A data were collected continuously in the middle estuarine zone at 0.32 m above the bed (fixed probe) and 0.2 m below the surface (floating probe) (Fig. 3). Some surface sampling was further conducted in the upper estuarine zone. Figure 6 presents the time-variations of water depth, specific conductivity, air and water temperature, pH and chlorophyll A in the middle and upper estuarine zones.

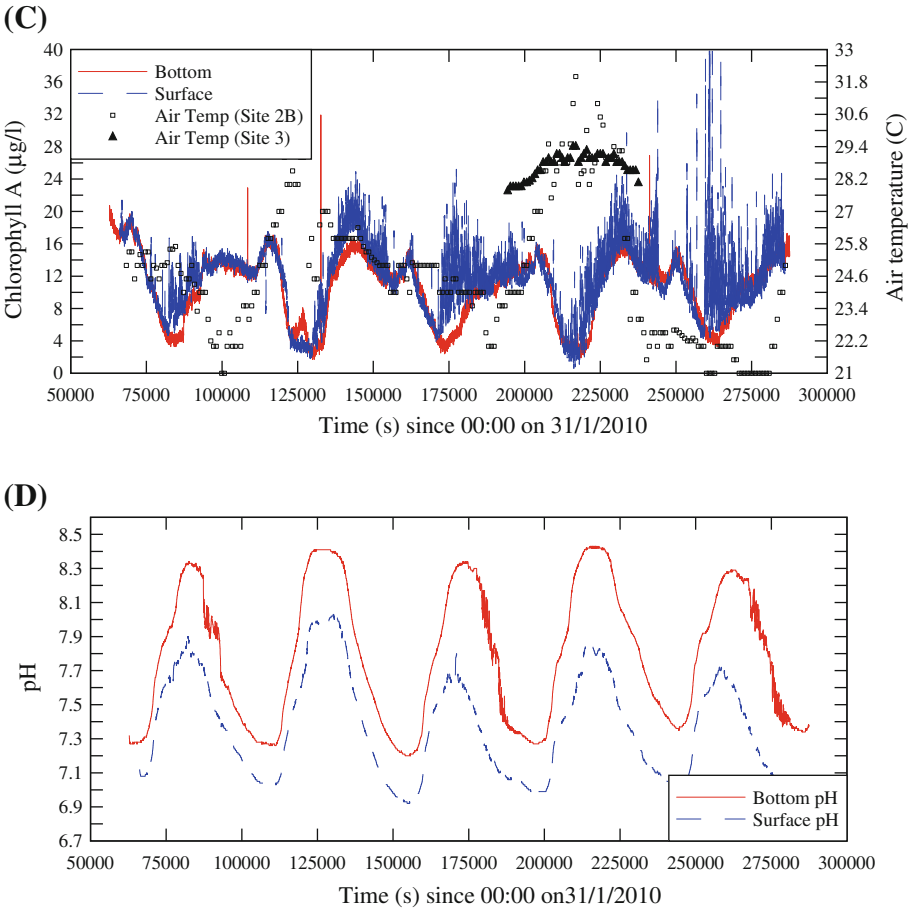

Fig. 6 contined

The water conductivity data showed a strong tidal trend, with maximum values at or very near high tide slack water following the flood tide in the middle estuary (Fig. 6a). The conductivity varied between 39.2 and 55.7, and 37.6 and 55.1 mS/cm at the bottom and next to the surface respectively. The middle estuary data showed very little stratification of the water column for the whole study period. The difference in conductivity across the depth was less than 2 mS/cm. This pattern was quite distinct from wet weather conditions when some vertical stratification was also observed [4,6]. The longitudinal variations in conductivity were further relatively limited. At Site 3, the water conductivity ranged from 29.2 to 44.1 mS/cm. Overall the conductivity ranges were comparable to an earlier study at the same sites during a relatively long drought period [6]. The time variations of water conductivity were mainly affected by tidal influences and to a lesser extent by freshwater inputs from the catchment and from sewage discharge.

The water temperature data showed a long-term decrease in temperature over the 4 days (Fig. 6b). The trend might be a combination of the effects of the colder freshwater runoff and the cooler-than-average weather conditions during the field study. There were some daily oscillations in water temperature that were likely linked with the diurnal air temperature

variations. The water turbidity data showed some marked peaks during the first half of the flood tide, as well as an unusual turbid event near the end of the flood tide around t = 125,700 s (Fig. 4b). Note that this unusual turbidity peak was associated with a relatively sudden increase in both bottom and surface water temperature data. Overall the turbidity data were close between the two YSI6600 probes. During the early flood tides, the turbidity readings reached values in excess of 80 to 100 NTU. These turbidity levels were large for Eprapah Creek, and significantly larger than during the earlier field studies conducted by the authors (Table 1).

The pH and DO data showed also a tidal trend with maximum values around high tide in the middle estuary. The pH readings varied between 7.2 and 8.43 at the bottom, and 6.92 and 8.03 next to the surface. The DO levels (not shown) varied between 57 and 99%, and 33 and 96% of saturation at the bottom and next to the surface respectively. The lowest pH level and DO content were observed at low tide slack systematically, and the maximum values were measured at high tide slack. The chlorophyll A data presented minimum values at the end of each flood tide, about 25 min on average before high tide (Fig. 6c).

Some vertical physio-chemical profiles were recorded at several longitudinal locations between the river mouth and the upper estuary on afternoon of 1 February 2010. Figure 7 presents some typical results in terms of water conductivity, temperature and turbidity; the data on the left were collected during the early ebb tide (HW + 1h to HW + 2h) and those on the right were recorded about mid ebb tide (LW - 4h to LW - 3h). On 1 February 2010, the estuarine zone was relatively well mixed in terms of specific conductivity, water temperature, pH and DO. The results were consistent with the YSI6600 probe data collected mid-estuary. The turbidity data suggested a reasonably well mixed water column during the early ebb tide (Fig. 7c1), but some larger turbidity levels were observed next to the bed during the mid ebb tide (Fig. 7c2). The finding was possibly linked with the greater vertical velocity gradient during the mid ebb tide. All other parameters showed relatively few vertical and longitudinal variations, while the temporal variations were consistent with earlier studies in Eprapah Creek [6].

3.3 Transient front and surface scars

A front is defined as an interface along which some water properties change abruptly [22]. Its presence may influence the horizontal dispersion and residual circulation, with significant impacts on the local chemical and biological processes [15,16,39]. Previously a major transient front was observed mid-estuary (Site 2B) during study E6 with neap tide conditions [30], and some mini-transient fronts were observed at the same site during the study E10 [33].

During the present study, a transient front was observed in the upper estuary (Site 3) during the early flood tide on 2 February 2010 between 08:27 and 09:30. Some surface slicks started to be seen at the upper estuarine site at 08:27 (t = 203,220 s) and developed progressively in a front which passed in front of Site 3 between 08:40 and 08:45. The front progressed slowly upstream and it was clearly seen up to 50 m upstream of Site 3 until 09:30 (Fig. 8). Figure 8 shows two photographs of the front advancing very slowly; note the line of debris progressing very slowly upstream.

Figure 9 presents the instantaneous velocity and surface sampling data at Site 3 between 08:15 and 09:45 including during the front passage. The surface sampling data suggested a 'spike' in surface water conductivity by about 8 mS/cm at about 08:45 (t = 204,300 s) corresponding to the formation and passage of the front at Site 3 (Fig. 9a, arrow). The ADV data showed some rapid and large turbulent velocity fluctuations during the front passage

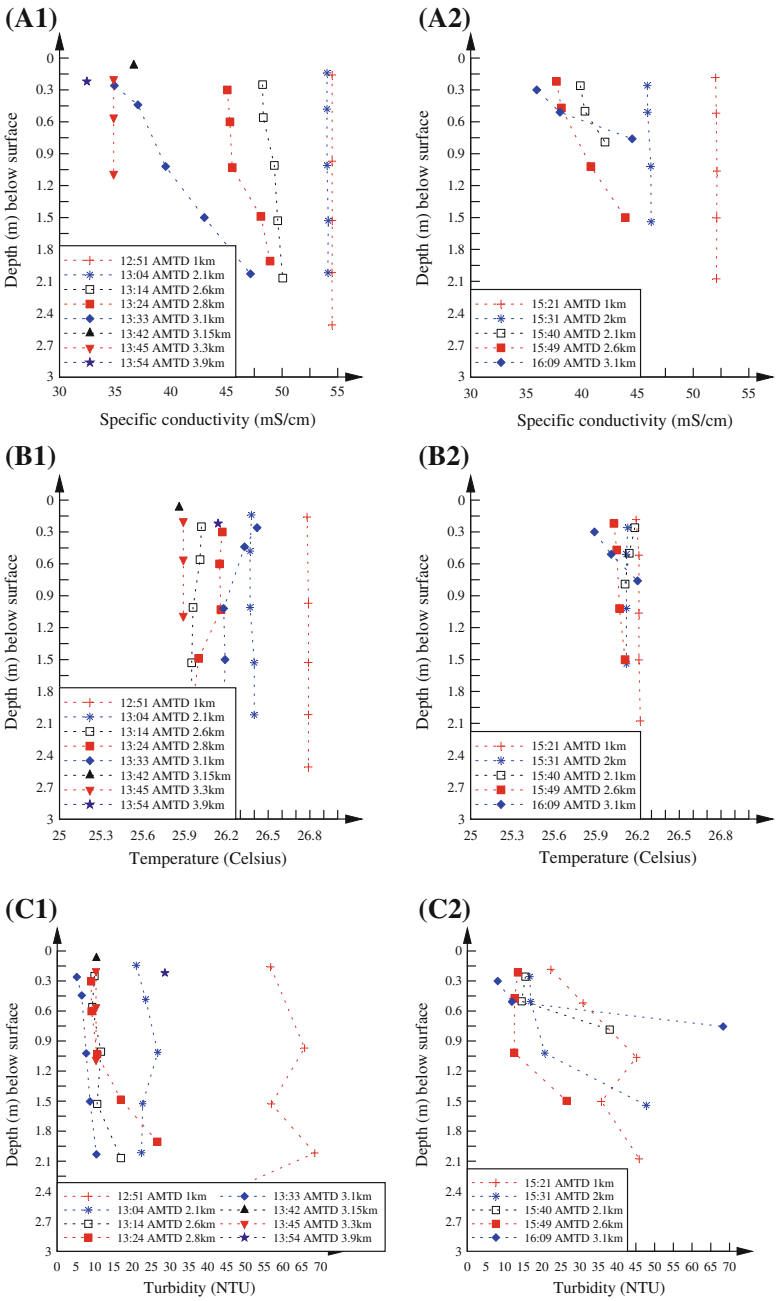

Fig. 7 Vertical profiles of physio-chemical properties. Data collected with a YSI6920 probe at Eprapah Creek on 1 February 2010 during the early ebb tide (*left*) and mid ebb tide (*right*). **a1** Specific conductivity during the early ebb tide. **a2** Specific conductivity during the mid ebb tide. **b1** Water temperature during the early ebb tide. **b2** Water temperature during the mid ebb tide. **c1** Turbidity during the early ebb tide. **c2** Turbidity during the mid ebb tide

Fig. 8 Transient front propagating upstream on 2 February 2010 in the upper estuary. Views from the right bank about 50 m upstream of Site 3 with the front progressing from *top right* to *bottom left* about 08:48

at about 08:41 (t = 204,600 s) for all components, with sustained fluctuations of all three velocity components for more than 25 min. Figure 9b and c shows both instantaneous and smoothed velocity data (500 data points window). The front propagation was associated with some intense secondary motion. After 08:41 (Fig. 9b, arrow), the surface and bottom waters (z = 0.24 m) flowed upstream until 08:54 (t = 204,840 s) before reversing and flowing downstream until 09:27. The fluctuations in vertical velocities showed some large amplitudes during the front passage and for the next 15 min (Fig. 9). The data showed some large velocity fluctuations and intense secondary motion during and shortly after the surface front passage. It was not possible to ascertain whether these were caused by the transient front, or whether the turbulent flow motion induced the formation of the transient front.

4 Turbulence properties in the middle estuary

In the small subtropical estuary of Eprapah Creek, the flow was turbulent and characterised by a broad spectrum of length and time scales. For the entire study, the relative elevation z/d of the sampling volume ranged from 0.04 to 0.86 (average 0.15) for the two ADV units located in the middle estuarine zone (Site 2B), where z is the sampling elevation above the bed and d is the flow depth. Thus the data were collected mainly in the outer flow region ($z/d > 0.1$) and any data scaling is based upon the outer flow properties.

The field observations showed systematically the large standard deviations of all velocity components during the flood and ebb tides (Figs. 5, 10). Figure 10 present the time variations of a few key turbulence parameters for a consecutive tidal cycle. (Herein a tidal cycle is defined as the period from a low tide to the next low tide, corresponding in fact to half a full

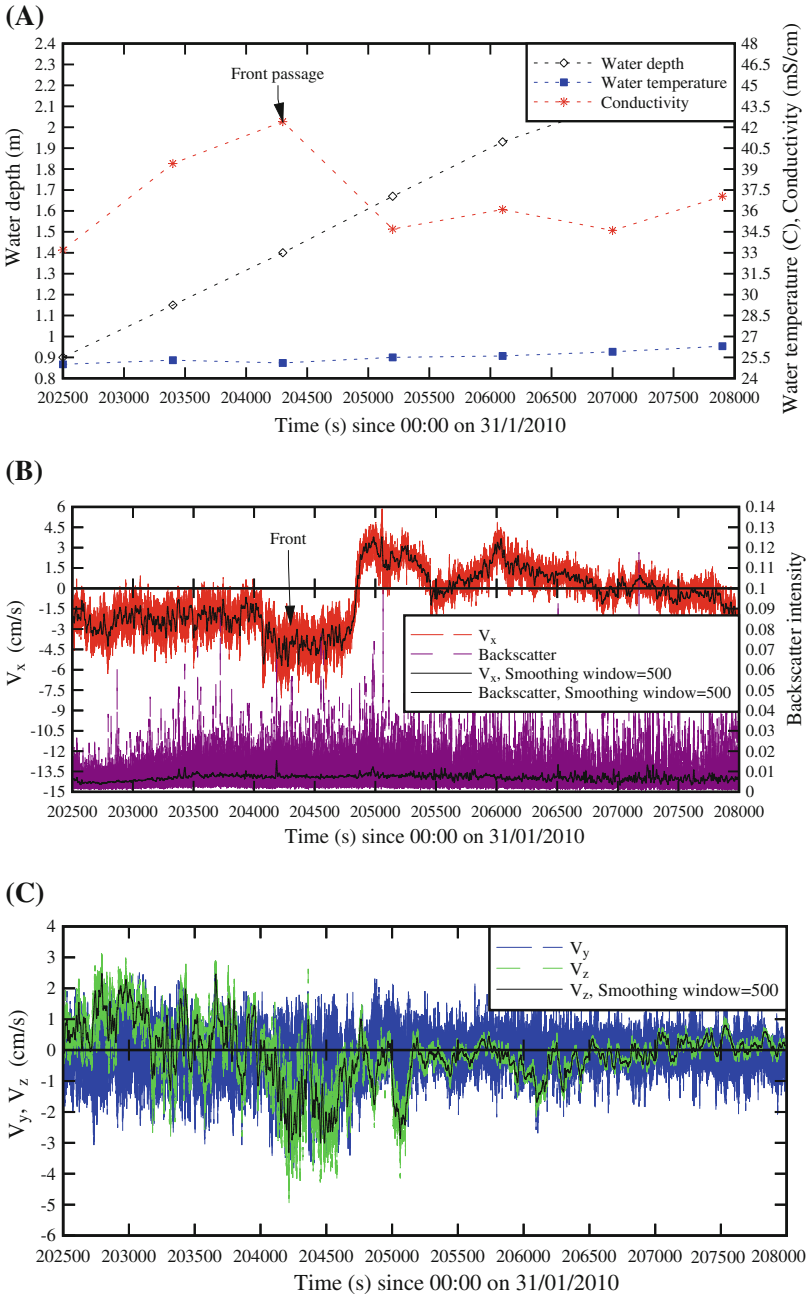

Fig. 9 Effect of the transient front passage on the turbulent flow properties at Site 3 (upper estuary) between 08:15 and 09:45. **a** Water depth and surface water temperature and conductivity. **b** Longitudinal velocity component V_x and acoustic BSI at z = 0.235 m (instantaneous data and smooth data (500 points window)). **c** Transverse velocity V_y and vertical velocity V_z components at z = 0.235 m (instantaneous data and smooth data (500 points window))

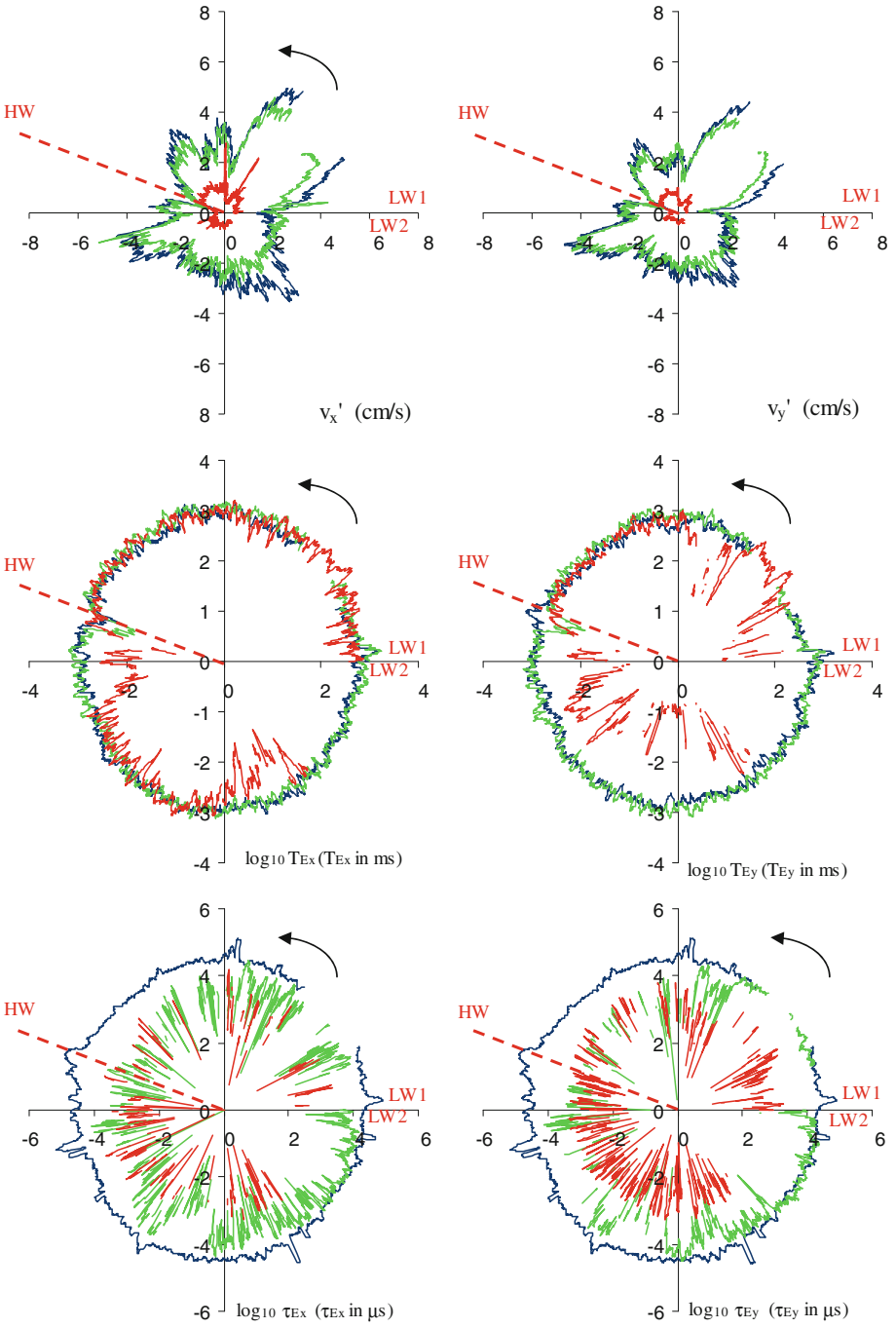

Fig. 10 Standard deviations of longitudinal and transverse velocity components v_x' and v_y', integral turbulent time scales T_{Ex} and T_{Ey}, and turbulent dissipation time scales τ_{Ex} and τ_{Ey} during a tidal cycle (t = 197,500 to 217,800 s). *Dark Blue* 0.12 m above bed at Site 2B, *bright green* 0.32 m above bed at Site 2B, *red* 0.235 m above bed at Site 3

semi-diurnal tidal cycle.) The data included the standard deviations of the longitudinal and transverse velocity components v'_x and v'_y, the integral turbulent time scales T_{Ex} and T_{Ey}, and the turbulent dissipation time scales τ_{Ex} and τ_{Ey}. Each graph shows the magnitude of the turbulent property calculated over 200 s from a low water (LW1) to the next low water (LW2), and the data are presented in a circular plot. The time variations of the data progress anti-clockwise and the high waters (HW) are indicated with a dashed red line. In each circular plot, the upper half corresponds to the flood tide, while the lower half is the ebb tide. For each figure, the dark blue data were sampled at 0.12 m above bed at Site 2B (mid-estuary), the bright green data were collected at 0.32 m above bed at Site 2B, and the red data were recorded at 0.235 m above bed at Site 3 (upper estuary). The longitudinal velocity V_x is positive downstream, and the transverse component V_y is positive towards the left bank. The full data sets for the entire field study are reported in [10].

Typical field measurements of standard deviations of the longitudinal velocity v'_x and transverse velocity v'_y are shown in Fig. 10 (top graphs). Figure 10 highlights the smaller velocity fluctuations during the end of the ebb tide and around the low tide slack, as well as the relatively large fluctuations in v'_x and v'_y overall. The vertical turbulence intensity v'_z/v'_x showed no discernable tidal trend.

Some time variations of integral turbulence time scales T_{Ex} and T_{Ey} are shown also in Fig. 10. Note that the axes have a logarithmic scale and the units are milliseconds. The integral time scales of streamwise velocity T_{Ex} were comparable during the flood and ebb tides (Fig. 10). The median values of the horizontal integral time scales T_{Ex} and T_{Ey} were 0.73 and 0.77, and 0.64 and 0.66 s respectively at 0.12 and 0.32 m above the bed. The dimensionless integral time scale T_{Ey}/T_{Ex} was about 0.85 on average at both elevations. [23] and [33] observed $T_{Ey}/T_{Ex} \sim 1.7$ and 1.0 in a tidal channel in Australia and mid-estuary of Eprapah Creek respectively, while [14] observed $T_{Ey}/T_{Ex} \sim 0.4$ in a rectangular laboratory channel.

The analysis of dissipation time scales of all velocity components showed no obvious trend with the tidal phase (Fig. 10). The turbulent dissipation time scale, or Taylor microscale, is a characteristic time scale of the smaller eddies which are primarily responsible for the dissipation of energy. The data yielded dissipation time scales $\tau_{Ex} \approx \tau_{Ey} \approx 30$ ms and 10 ms at $z = 0.12$ and 0.32 m above the bed respectively. The dimensionless transverse dissipation time scale was on average $\tau_{Ey}/\tau_{Ex} = 1.0$ and 1.6 at 0.12 and 0.32 m above the bed respectively. For comparison, [14] obtained $\tau_{Ey}/\tau_{Ex} \sim 0.9$ in a rectangular laboratory channel.

The median turbulent time scale data are shown in Table 2. Table 2 lists the end and start times of each of the five tidal cycles investigated during the study (columns 3 and 4). The low and high water times were based upon the water elevation measurements at Site 2B (mid-estuary). In Table 2, the columns 5–22 (Table 2) present the median value of each turbulence time scale at Site 2B (ADV UQ & ADV QUTD) and at Site 3 (ADV QUTS). The observations at Site 2B showed some comparable results at $z = 0.12$ and 0.32 m, while the data in the upper estuary (Site 3) yielded systematically smaller integral turbulence time scales T_{Ey}. Overall, the results were very close for the duration of the field study between the tidal cycles TC1–TC5 (Table 2).

The tangential Reynolds stresses varied with the tide during the field work. Figure 11 illustrates the variations with time of the time-averaged turbulent stresses $\rho \times \overline{v_x \times v_y}$ and $\rho \times \overline{v_x \times v_z}$ for the entire field study. The tangential stress $\rho \times \overline{v_x \times v_y}$ was the largest about low tide, just before and just after low tide slack (Fig. 11a). The tangential stress $\rho \times \overline{v_x \times v_z}$ was predominantly positive during the flood tide and negative during the ebb tide (Fig. 11b). Figure 11 includes also the data collected at Site 3 on 2 February 2010. The time-averaged

Table 2 Median turbulent time scales during each tidal cycle of the field study E11 at Eprapah Creek between the 31 January and 3 February 2010

Tidal cycle	Date	Start time	End time	T_{Ex}			T_{Ey}		
		LW1	LW2	ADV UQ	ADV QUTD	ADV QUTS	ADV UQ	ADV QUTD	ADV QUTS
		s	s	s	s	s	s	s	s
(1)	(2)	(3)	(4)	(5)	(6)	(7)	(8)	(9)	(10)
TC1	31/1/2010–1/2/2010	66,300	108,900	0.747	0.691	–	0.666	0.625	–
TC2	1/2/2010	108,900	154,800	0.765	0.861	–	0.608	0.688	–
TC3	1–2/2/2010	154,800	197,500	0.714	0.605	–	0.634	0.577	–
TC4	2/2/2010	197,500	243,900	0.779	0.849	0.699	0.627	0.724	0.291
TC5	2–3/2/2010	243,900	285,700	0.659	0.861	–	0.641	0.688	–

Tidal cycle	τ_{Ex}			τ_{Ey}			T_{Ey}/T_{Ex}			τ_{Ey}/τ_{Ex}		
	ADV UQ	ADV QUTD	ADV QUTS	ADV UQ	ADV QUTD	ADV QUTS	ADV UQ	ADV QUTD	ADV QUTS	ADV UQ	ADV QUTD	ADV QUTS
	s	s	s	s	s	s						
(1)	(11)	(12)	(13)	(14)	(15)	(16)	(17)	(18)	(19)	(20)	(21)	(22)
TC1	0.0425	0.0059	–	0.0430	0.0141	–	0.87	0.90	–	1.01	1.66	–
TC2	0.0280	0.0071	–	0.0284	0.0115	–	0.80	0.79	–	1.01	1.57	–
TC3	0.0371	0.0059	–	0.0374	0.0110	–	0.88	0.93	–	1.01	1.72	–
TC4	0.0297	0.0059	0.0007	0.0300	0.0141	0.0007	0.81	0.84	0.48	1.01	1.66	0.93
TC5	0.0357	0.0071	–	0.0358	0.0115	–	0.95	0.79	–	1.00	1.57	–

Notes. Times since 00:00 on 31/1/2010; low and high water times are based upon the water elevation measurements at Site 2B (mid-estuary); *ADV UQ & ADV QUTD* located at Site 2B (mid-estuary) at z = 0.12 and 0.32 m respectively; *ADV QUTS* located at Site 3 (upper estuary) at z = 0.235 m; (–) data not available

tangential stresses were one order of magnitude smaller in the upper estuarine zone. Smaller Reynolds stresses indicated reduced mixing in the upper estuary.

The standard deviations of the tangential Reynolds stresses showed some significant fluctuations and were the largest during the early flood tide. Table 3 presents the median tangential stress data together with the standard deviations of the turbulence velocity components. On average, the dimensionless tangential stress fluctuations were equal to $(v_x \times v_z)'/(v'_x \times v'_x) \approx (v_x \times v_y)'/(v'_x \times v'_x) \approx 1.1$ to 1.25 respectively in the middle estuarine zone (Site 2B) and in the upper estuary (Site 3). For comparison, some laboratory observations in a straight prismatic rectangular channel yielded $(v_y \times v_x)'/(v'_x \times v'_x) \sim 1.0$ to 1.6 [14].

4.1 Discussion: shear stress and secondary currents

The boundary shear stress was estimated from the velocity gradient next to the bed, although other techniques may be used [5,27,17]. The near-bed velocity shear stress was calculated as:

$$\tau_o = \rho \times \left(\kappa \times \frac{V_1}{\mathrm{Ln}\frac{z_1}{K_s}} \right)^2 \quad (3)$$

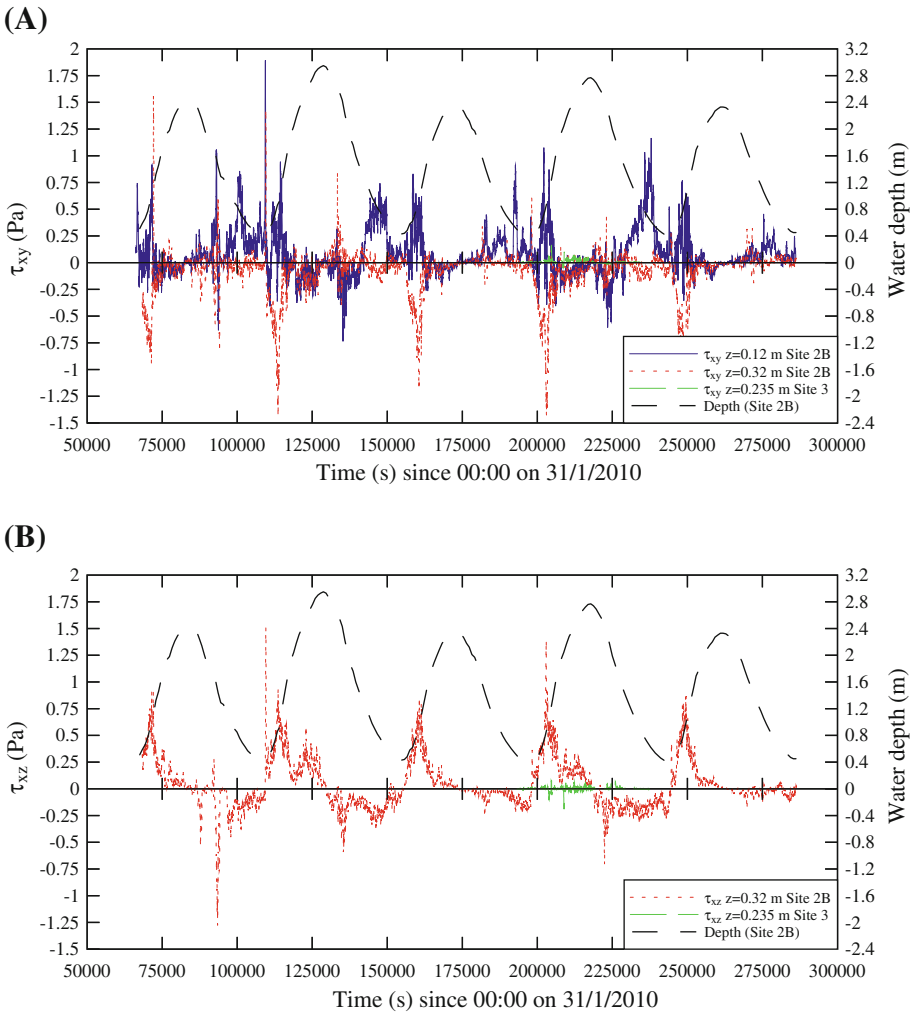

Fig. 11 Water depth and time-averaged tangential Reynolds stresses as functions of time. *Dark blue* 0.12 m above bed at Site 2B, *bright green* 0.32 m above bed at Site 2B, *red* 0.235 m above bed at Site 3. Data collected in Eprapah Creek during the study E11 (31 June–3 February 2010). VITA calculations using the average of the next 10,000 samples (200 s) at 10 s intervals along entire data sets. **a** $\rho \times \overline{v_x \times v_y}$ and **b** $\rho \times \overline{v_x \times v_z}$

where ρ is the fluid density, V_1 is the time-averaged longitudinal velocity measured at $z = z_1$ ($z_1 = 0.12$ m, Study E11), κ is the von Karman constant ($\kappa = 0.4$) and k_s is the equivalent roughness height. At the middle estuarine site 2B, the river bed consisted of gravels and sharp rocks (Fig. 3a) corresponding to $k_s \approx 10$ mm. For the entire field study, the median shear stress was $\tau_o = 0.158$ Pa. The boundary shear stress was the greatest during the early flood tide when the measured longitudinal velocity amplitude was the largest (Fig. 4a).

The boundary shear stress data may be compared with the tangential Reynolds stress $\rho \times \overline{v_x \times v_z}$ measured at $z = z_2$ ($z_2 = 0.32$ m, Study E11), as well as with the velocity gradient shear stress, measured between the two ADV units located at $z = z_1$ and $z = z_2$, and defined as

Table 3 Median standard deviations of the turbulent velocity components and tangential Reynolds stresses during the field study E11 at Eprapaph Creek between the 31 January and 3 February 2010

Site	ADV Unit	z m	v'_x m/s	v'_y m/s	v'_z m/s	$\rho \times (v_x \times v_y)'$ Pa	$\rho \times (v_x \times v_z)'$ Pa	$\rho \times (v_y \times v_z)'$ Pa
(1)	(2)	(3)	(4)	(5)	(6)	(7)	(8)	(9)
2B	ADV UQ	0.12	0.0238	0.0215	–	0.576	–	–
	ADV QUTD	0.32	0.0220	0.0206	0.0180	0.485	0.442	0.395
3	ADV QUTS	0.235	0.0052	0.0037	0.0024	0.024	0.016	0.010

Table 4 Comparison in median shear stress in the middle estuary of Eprapah Creek (Site 2B, AMTD 2.1 km)

Parameter (1)	Field study E10 (2)	Field study E11 (3)	Units (4)	Remarks (5)
Maximum tidal range	1.76	2.78	m	
Study period	50	60	h	Sampling period
Sampling rate	50	50	Hz	Continuous sampling rate
z_1	0.13	0.12	m	
z_2	0.38	0.32	m	
τ_o	0.0052	0.158	Pa	Equation 3 median value
τ_{12}	0.052	0.326	Pa	Equation 4 median value
$\rho \times \overline{v_x \times v_z}(z = z_2)$	0.02	0.118	Pa	Median value of absolute value
$\rho \times \overline{v_x \times v_y}(z = z_1)$	0.024	0.092	Pa	Median value of absolute value
$\rho \times \overline{v_x \times v_y}(z = z_2)$	0.031	0.049	Pa	Median value of absolute value

$$\tau_{12} = \rho \times \left(\kappa \times \frac{V_2 - V_1}{Ln \frac{z_2}{z_1}} \right)^2 \quad (4)$$

For the entire field study, the median tangential stress magnitude and the median velocity gradient shear stress were respectively $\rho \times \overline{v_x \times v_z} = 0.12$ and $\tau_{12} = 0.326$ Pa. For comparison, the median tangential shear stresses $\rho \times \overline{v_x \times v_y}$ measured by the two ADV units were 0.092 Pa and 0.050 Pa at z = 0.12 and 0.32 m respectively. The present results are summarised in Table 4 where they are compared with earlier results obtained at the same sampling site and similar elevations under neap tide conditions.

The findings implied that the turbulence shear stresses measured at 0.12 m < z < 0.32 m were comparable to the boundary shear stress (Eq. 3) with king tide conditions. The observations differed from the turbulence data measured under neap tide conditions (Table 4, column 2). It is believed that the comparative data implied the relatively larger three-dimensional effects associated with the existence of strong secondary currents under neap tide conditions (Study E10).

During the present study, some anomalies were observed in terms of the transverse velocity data. For some periods, the time-averaged transverse velocities V_y recorded at $z = z_1 = 0.12$ and $z = z_2 = 0.32$ m flowed in opposite directions for relatively long periods (e.g. Fig. 12a). Such anomalies were observed during the flood and ebb tides, and around high tide slack for the entire study. For other longer periods, the transverse velocity V_y at $z = z_1 = 0.12$ m flowed in the same direction as, but with a greater magnitude than, at the higher elevation

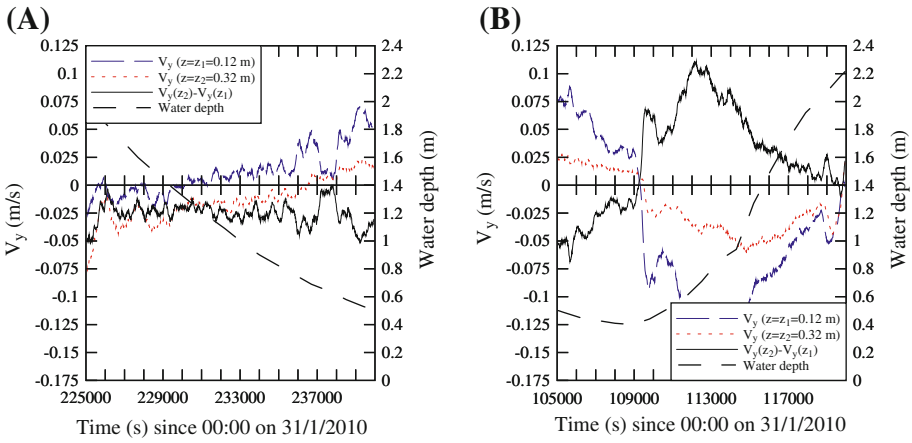

Fig. 12 Transverse shear flow patterns at the middle estuary sampling site 2B: time-variations of the time-averaged transverse velocities for the lower ADV ($z_1 = 0.12$ m) and upper ADV ($z_2 = 0.32$ m) units, time-averaged transverse velocity gradient ($V_y(z = z_2) - V_y(z = z_1)$) and water depth during the study E11. **a** Mid ebb tide on 2 February 2010 and **b** flood tide on 1 February 2010

$z_2 = 0.32$ m (e.g. Fig. 12b). This second kind of anomaly was recorded during the flood tide and at the end of the ebb tide. These observations suggested the occurrence of some secondary currents associated with strong transverse shear and large tangential stresses $\rho \times v_x \times v_y$ at the sampling location. Figure 12a shows the time-averaged transverse velocity data V_y together with the time-averaged transverse velocity difference during a mid ebb tide period. Here V_y is positive towards the left bank. Figure 12a presents about 4 h 10 min of samples with a large transverse shear event between about t = 230,000 and 236,000 s when the transverse velocities V_y recorded at z = 0.12 and 0.32 m above the bed flowed in opposite directions: i.e., towards the left and right banks respectively. Figure 12b presents about 4 h 10 min of samples during the flood tide when the transverse velocity magnitude at $z_1 = 0.12$ m was significantly larger than that at $z_2 = 0.32$ m between about t = 109,350 and 119,350 s.

The velocity standard deviation data yielded $v'_y/v'_x \sim 0.9$ throughout the study while $v'_z/v'_x \sim 0.75$. The findings were close to recent LES computations in a shallow water channel with similar Reynolds number conditions [12]. Note that the results $v'_z < v'_x$ implied some turbulence anisotropy. Trevethan [29] discussed the formation of the transverse velocity anomalies in Eprapah Creek, their collapse, and their reformation in the opposite direction. He suggested that the alternation in transverse shear anomalies was linked with the long period oscillations induced by outer resonance. The present longitudinal velocity data (Fig. 4a) showed some seiching under the king tide conditions that were linked possibly with some East-West resonance in the Moreton Bay.

5 Conclusion

Some detailed turbulence field measurements were conducted in a small subtropical estuary with semi-diurnal tides during king tide conditions: i.e., the tidal range was 2.78 m, the largest for both 2009 and 2010. The velocity measurements were performed continuously at high frequency (50 Hz) for 60 h and the data complemented a series of earlier studies in the same micro-tidal estuarine system, mostly conducted under neap tides (Table 1). Herein two ADVs

were sampled simultaneously in the middle estuarine zone at z = 0.12 and 0.32 m above the bed for the entire study duration. A third acoustic Doppler velocimeter was deployed in the upper estuary and sampled continuously at 50 Hz for 12 h within the study period.

Under the king tide conditions the extreme low and high water levels had some impact on the estuary hydrodynamics. At high tides, the mangroves and surrounding mudflats were inundated. During the early ebb tide, the estuary cross-section was drastically reduced when the water level dropped below the river bank edges. The mangrove swamps and flats continued to trap some brackish waters that were released into the creek during the later stages of the ebb tide. At low tides, some rock formations, shoals and bars created some flow disruption between the upper and lower estuarine zones. The upper estuarine zone became practically disconnected from the lower estuary. The water column was well mixed throughout the study period, but the turbidity levels during king tides were significantly larger than those recorded during the earlier field studies under neap and spring tides. A transient front was observed in the upper estuary during the early flood tide on 2 February 2010. The surface sampling data suggested a surge in surface water conductivity during the formation and passage of the front, while the ADV data showed a sudden increase in turbulent velocity fluctuations with fluctuations of all three velocity components sustained for more than 25 min.

The continuous turbulent velocity sampling at high frequency provided a detailed characterisation of the time-variations of turbulence field. The rapid and large fluctuations in all turbulent properties during a whole tidal cycle were a prominent aspect of the estuarine flow motion. Overall the present data showed some marked differences between king tide and neap tide conditions. During king tides, the tidal forcing was the dominant water exchange and circulation mechanism in the estuary. In contrast, the long-term oscillations linked with internal and external resonance played a major role in the turbulent mixing during neap tides. The data sets showed further the upper estuarine zone is drastically less affected by the spring tide range; the flow motion remained slow, but the present turbulent velocity data were clearly affected by the propagation of a transient front during the very early flood tide motion at that sampling site.

Acknowledgments The authors thank all the people who participated in the field work and without whom the study could not have been conducted. They thank Dr Jon Hinwood (Monash University, Australia) for his valuable comments. They acknowledge the support and assistance of Dr Dave Rissik, Dr Ian Ramsay and John Ferris (Qld DERM), as well as the assistance of Brad Taylor and Sonja Toft (Redland Shire Council), and Mrs Lynn Roberts (ECCLA).

References

1. Bowden KF, Ferguson SR (1980) Variations with height of the turbulence in a tidally-induced bottom boundary layer. In: Nihoul JCJ (ed) Marine turbulence. Elsevier, Amsterdam The Netherlands, pp 259–286
2. Bowden KF, Howe MR (1963) Observations of turbulence in a tidal current. J Fluid Mech 17(2):271–284
3. Chanson H (2004) Environmental hydraulics of open channel flows. Elsevier Butterworth-Heinemann, Oxford. ISBN 0-7506-6165-8
4. Chanson H (2008) Field observations in a small subtropical estuary during and after a rainstorm event. Estuar Coastal Shelf Sci 80(1):114–120. doi:10.1016/j.ecss.2008.07.013
5. Chanson H (2009) Applied hydrodynamics: an introduction to ideal and real fluid flows. CRC Press/Balkema/Taylor & Francis Group, Leiden
6. Chanson H, Ramsay I (2008) Spatial variations in physio-chemistry in a small sub-tropical river estuary. In: Water Management, Proceedings of the Institution of Civil Engineers, UK, vol 161, No. WM5, pp 241–251 & Cover photograph. doi:10.1680/wama.2008.161.5.241

7. Chanson H, Brown R, Ferris J, Ramsay I, Warburton K (2005) Preliminary measurements of turbulence and environmental parameters in a sub-tropical estuary of Eastern Australia. Environ Fluid Mech 5(6):553–575. doi:10.1007/s10652-005-0928-y
8. Chanson H, Trevethan M, Aoki S (2008) Acoustic Doppler velocimetry (ADV) in small estuary : field experience and signal post-processing. Flow Meas Instrum 19(5):307–313. doi:10.1016/j.flowmeasinst.2008.03.003
9. Chanson H, Takeuchi M, Trevethan M (2008) Using turbidity and acoustic backscatter intensity as surrogate measures of suspended sediment concentration in a small sub-tropical estuary. J Environ Manag 86(4):1406–1416. doi:10.1016/j.jenvman.2007.07.009
10. Chanson H, Brown R, Trevethan M (2010) Turbulence measurements in a small subtropical estuary under king tide conditions. Hydraulic Model Report No. CH77/10, School of Civil Engineering, The University of Queensland, Brisbane, Australia, 82 pp. ISBN 9781864999969
11. Henderson FM (1966) Open channel flow. MacMillan Company, New York
12. Hinterberger C, Fröhlich J, Rodi W (2008) 2D and 3D turbulent fluctuations in open channel flow with $Re_\tau = 590$ studied by large eddy simulation. Flow Turbul Combust 80(2):225–253. doi:10.1007/s10494-007-9122-2
13. Kawanisi K, Yokosi S (1994) Mean and turbulence characteristics in a tidal river. Cont Shelf Res 17(8):859–875
14. Koch C, Chanson H (2009) Turbulence measurements in positive surges and bores. J Hydraul Res IAHR 47(1):29–40. doi:10.3826/jhr.2009.2954
15. Largier JL (1992) Tidal intrusion fronts. Estuaries 15(1):26–29
16. Largier JL (1993) Estuarine fronts : how important are they?. Estuaries 16(1):1–11
17. Montes JS (1998) Hydraulics of open channel flow. ASCE Press, New York
18. Neal C, House WA, Leeksa GJL, Whitton BA, Williams RJ (2000) Conclusions to the special issue of Science of the total environment concerning 'The water quality of UK rivers entering the North Sea'. Sci Tot Environ 251:557–573
19. Nezu I (2005) Open-channel flow turbulence and its research prospect in the 21st century. J Hydraul Eng ASCE 131(4):229–246
20. Nezu I, Nakagawa H (1993) Turbulence in open-channel flows. IAHR Monograph. IAHR Fluid Mechanics Section, Balkema Publication, Rotterdam
21. Nikora V, Goring D (2002) Fluctuations of suspended sediment concentration and turbulent sediment fluxes in an open-channel flow. J Hydraul Eng ASCE 128(2):214–224
22. Officer CB (1976) Physical oceanography of estuaries (and associated coastal waters). Wiley, New York
23. Osonphasop C (1983) The measurements of turbulence in tidal currents. PhD thesis, Department of Mechanical Engineering, Monash University, Australia
24. Ralston DK, Stacey MT (2005) Stratification and turbulence in subtidal channels through intertidal mudflats. J Geophys Res Oceans AGU 110:Paper C08009
25. Savenije HHG (1993) Composition and driving mechanisms of longitudinal tidal average salinity dispersion in estuaries. J Hydrol 144:127–141
26. Savenije HHG (2005) Salinity and tides in alluvial estuaries. Elsevier, Amsterdam
27. Schlichting H (1979) Boundary layer theory, 7th edn. McGraw-Hill, New York
28. Shiono K, West JR (1987) Turbulent perturbations of velocity in the conwy estuary. Estuar Coastal Shelf Sci 25:533–553
29. Trevethan M (2008) A fundamental study of turbulence and turbulent mixing in a small subtropical estuary. PhD thesis, Department of Civil Engineering, The University of Queensland
30. Trevethan M, Chanson H (2007) Detailed measurements during a transient front in a small subtropical estuary. Estuar Coastal Shelf Sci 73(3–4):735–742. doi:10.1016/j.ecss.2007.03.014
31. Trevethan M, Chanson H (2009) Turbulent mixing in a small estuary: detailed measurements. Estuar Coastal Shelf Sci81(2):191–200. doi:10.1016/j.ecss.2008.10.020
32. Trevethan M, Chanson H, Takeuchi M (2007) Continuous high-frequency turbulence and sediment concentration measurements in an upper estuary. Estuar Coastal Shelf Sci 73(1–2):341–350. doi:10.1016/j.ecss.2007.01.014
33. Trevethan M, Chanson H, Brown R (2008) Turbulence characteristics of a small subtropical estuary during and after some moderate rainfall. Estuar Coastal Shelf Sci 79(4):661–670. doi:10.1016/j.ecss.2008.06.006
34. Uncles RJ (2003) From catchment to coastal zone: examples of the application of models to some long-term problems. Sci Tot Environ 314:567–588
35. van der Ham R, Fromtijn HL, Kranenburg C, Winterwerp JC (2001) Turbulent exchange of fine sediments in a tidal channel in the Ems/Dollard estuary. Part I. Turbulence measurements. Cont Shelf Res 21:1605–1628

36. Vanzoest R, Vaneck GTM (1991) Occurrence and behavior of several groups of organic micropollutants in the Scheldt estuary. Sci Tot Environ 103(1):57–71
37. Voulgaris G, Meyers ST (2004) Temporal variability of hydrodynamics, sediment concentration and sediment settling in a tidal creek. Cont Shelf Res 24:1659–1683
38. West JR, Oduyemi KOK (1989) Turbulence measurements of suspended solids concentration in estuaries. J Hydraul Eng ASCE 115(4):457–473
39. Wolanski E, Hamner WM (1988) Topographically controlled fronts in the ocean and their biological influence. Science 241:177–181